



### **Science Arts & Métiers (SAM)**

is an open access repository that collects the work of Arts et Métiers Institute of Technology researchers and makes it freely available over the web where possible.

This is an author-deposited version published in: <https://sam.ensam.eu>  
Handle ID: <http://hdl.handle.net/10985/15684>

#### **To cite this version :**

Côme LEGRAND, Guillaume FROMENTIN, Gerard POULACHON, Richard CHATAIN, Mickaël RANCIC - A geometrical and mechanistic generalized model for complex shape broaching of super alloy - In: 17th CIRP Conference on Modeling of Machining Operations, Royaume-Uni, 2019-06 - Procedia CIRP - 2019

Any correspondence concerning this service should be sent to the repository

Administrator : [scienceouverte@ensam.eu](mailto:scienceouverte@ensam.eu)



17th CIRP Conference on Modelling of Machining Operations

## A geometrical and mechanistic generalized model for complex shape broaching of super alloy

Côme LEGRAND<sup>\*ab</sup>, Guillaume FROMENTIN<sup>a</sup>, Gérard POULACHON<sup>a</sup>,  
Richard CHATAIN<sup>a</sup>, Mickaël RANCIC<sup>b</sup> \*

<sup>a</sup> Arts et Metiers ParisTech, LaBoMaP, UBFC, F-71250 Cluny, France

<sup>b</sup> Safran Aircraft Engines, Rue Henri Auguste Desbrières, F-91000 Évry, France

\* Corresponding author. Tel.: +33 3 85 59 53 88. E-mail address: [come.legrand@ensam.eu](mailto:come.legrand@ensam.eu)

### Abstract

The aircraft engine disks are highly critical parts. It is required for blade assembly to obtain high quality slots after broaching. Because of the complexity of the slot shapes, different problems are induced such as the cutting geometry, the broach design and the difficulties to evaluate the forces applied on the tool. To deal with this problematic, this article presents a geometrical and mechanistic model taking into account the various geometrical parameters of a form broach (pitch, shift, profiles and cutting geometry of the half teeth) to determine the cutting forces. The methodology of the cutting edges discretization and an oblique cutting law have been used. Several simulations made with this generalized model are presented to understand the impacts of the variation of the tool's geometrical parameters on the cutting forces evolution in order to improve the broaching of complex shape.

© 2019 The Authors. Published by Elsevier B.V.

Peer-review under responsibility of the scientific committee of The 17th CIRP Conference on Modelling of Machining Operations, in the person of the Conference Chair Dr Erdem Ozturk and Co-chairs Dr Tom Mcleay and Dr Rachid Msaoubi.

**Keywords:** Broaching; Modelling; Complex shape; Super alloy.

### 1. Introduction

Broaching is a process allowing to generate complex shape with accuracy, good surface integrity and high productivity. These are the reasons why broaching is used in aerospace to produce critical part such as turbine disk slots. However, it is a complex process and only few researches have been conducted on the subject in the known literature [1]. The main concerns are the local geometry variation all along the cutting edges (rake, inclination, clearance angles...), the local forces magnitude evolution applied on each cutting edge and the unbalance of the forces applied on the broach, in the case of angled disks machining. The choice of a suitable broaching strategy to obtain an optimised process is also not obvious to determine.

This study presents a parametrized model taking into account various parameters such as the pitch, the half teeth

alternation (shift), the orientation of the rake faces and the directions of the flank faces. The methodology of the cutting edges discretization with a local cutting law is used to calculate the local and global cutting forces applied on the tool. This methodology was made possible by the work of Sabberwal [2] and is now commonly used for other machining technics [3-6]. Vogel et al. [7] present results of a model for cutting force calculation applied to broaching but for rectilinear cutting edges and only taking into account the rake angle as parameters of the local geometry. Vogel et al. [8] made a broach design software but the methodology is not detailed in this article and only the cutting force along the broach axis is calculated.

This study has for objective to go further, taking into account complex shape broaching and considering more geometrical parameters of a broaching tool. Moreover, the three cutting forces components are predicted.

## 2. Global geometrical parametrization of broaching

### 2.2. Parametrization

The parametrization of a broaching operation is presented in Fig. 1. The model may consider an inclination angle (WPI) between the broach and the part axis. In addition, the number of half teeth, the variable pitches and the shift are configured.

#### Nomenclature

##### Broach parameters:

**Tooth** or **Pair of half teeth**: The two half teeth with symmetrical profiles on both side of the broach.

**Pitch**: distance between two half teeth on the same side of the broach (mm).

**Shift**: Distance between two half teeth of a pair, if the half teeth are alternated (mm).

**Z<sub>ab</sub>**: Half teeth of the pair number a ( $a \in [1, 5]$  in this case), on the right or left side of the broach considering the displacement direction ( $b \in [R, L]$ ). The first pair of half teeth is the first one entering into the part when machining.

**WPI**: Workpiece inclination angle between the broach and the part axis ( $^\circ$ ).

**v<sub>c</sub>**: Cutting speed of the broach (m/min).

**RPT**: Rise Per Tooth (mm).

##### Cutting geometry parameters:

**$\gamma_n$** : Normal rake angle at the considered point ( $^\circ$ ).

**$\lambda_s$** : Cutting edge inclination angle at the considered point ( $^\circ$ ).

**$\alpha_n$** : Normal clearance angle at the considered point ( $^\circ$ ).

**$\gamma_{n0}$** : Normal rake angle used to define the rake face orientation ( $^\circ$ ).

**$\lambda_{s0}$** : Cutting edge inclination angle used to define the rake face orientation ( $^\circ$ ).

**Ag**: Angle of the grinding direction between the vertical (Y axis) and the grinding wheel axis ( $^\circ$ ).

**Af**: Angle of the flank face tangential vector (Af) between the cutting speed of the broach and the displacement direction of the grinding wheel ( $^\circ$ ).

##### Force model parameters:

**h**: cut thickness (mm).

**$\Phi_{\text{shear}}$** : Shear angle ( $^\circ$ ).

**$\tau_s$** : Maximum shear stress (MPa).

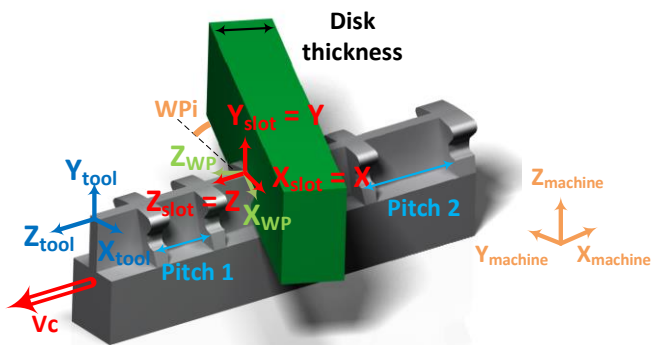


Fig. 1. Parametrization of a broaching operation.

The study is focused on a finishing operation. The rises per tooth are considered to be constant and equal to 0.1 mm, perpendicularly to the final slot profile. All the profiles are presented on Fig. 2.

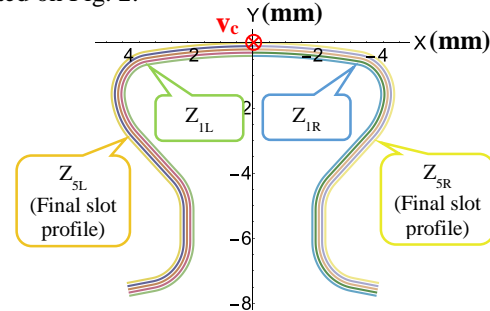


Fig. 2. Superposition of the half teeth profiles. Left and right sides are considered from the cutting speed direction.

### 2.2. Geometrical modelling

The developed methodology allows, thanks to the knowledge of the half teeth profiles and the orientation of the rake faces in particular points, to calculate the local cutting geometry for each point of the cutting edges. The different steps of the methodology are presented on Fig. 3. This methodology has been used by Fromentin et al. [9] for another machining operation.

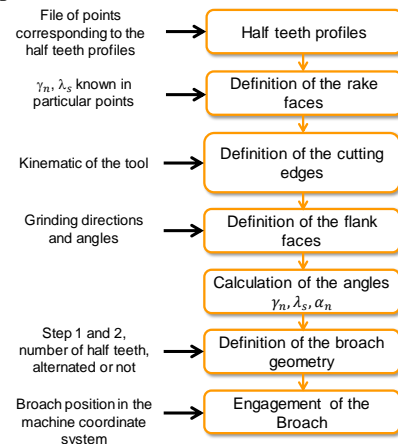


Fig. 3. Methodology used for the geometrical model definition.

This methodology gives a parametrized geometrical model. The orientations of the rake faces are defined by two angles ( $\gamma_n$  and  $\lambda_s$ ) in particular points. These points are defined by the intersection of the median plane of the broach and the half teeth profiles. The angles are called  $\gamma_{n0}$  and  $\lambda_{s0}$ , they are parametrized on Fig. 4.

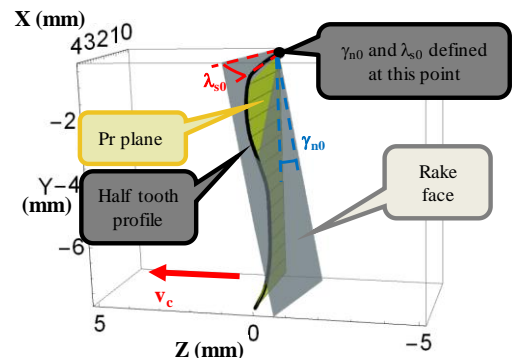


Fig. 4. Definition of a rake face. Example with  $\gamma_{n0}$  and  $\lambda_{s0}$  equal to  $10^\circ$ .

The grinding process generates plane rake faces. It implies that the local geometries all along the cutting edges are different than  $\gamma_{n0}$  and  $\lambda_{s0}$ . Then the half teeth profiles in the reference plane (Pr), orthogonal to  $v_c$ , are projected on the rake faces along the cutting speed direction. The cutting edges are obtained on Fig. 5.

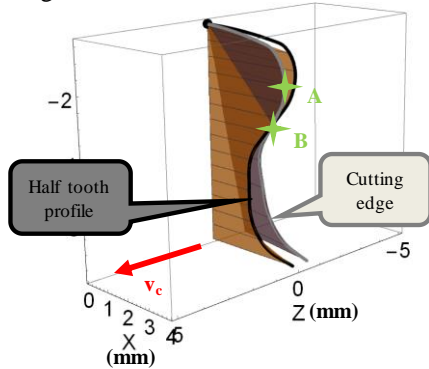


Fig. 5. Definition of a cutting edge. A and B are two reference points for Fig. 7.

The orientations of the flank faces are defined by the grinding parameters Af and Ag presented on Fig. 6.

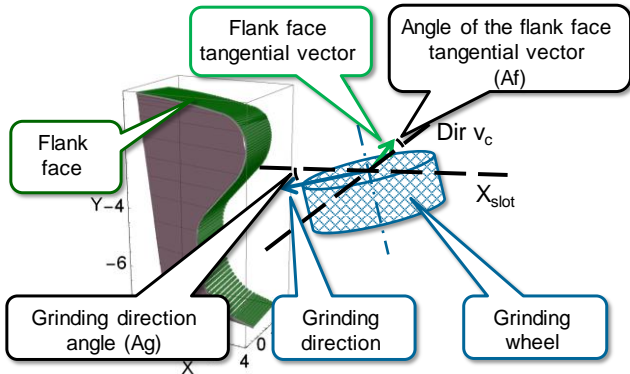


Fig. 6. Definition of the flank faces.

It is now possible to calculate the local cutting geometry at each point of the cutting edges according to the standard ISO 3002. Fig. 7 represents (in black colour) a half tooth profile and the different angles of the cutting geometry as a function of the vertical axis of the profile. The local cutting geometry depends on the rake face orientation ( $\gamma_{n0}$  and  $\lambda_{s0}$ ).

Knowing the cutting edge, the rake and flank faces of each half tooth, it is now possible to design the broach, locating the half teeth at a distance equal to the different pitches. The modelled broach is presented on Fig. 8.

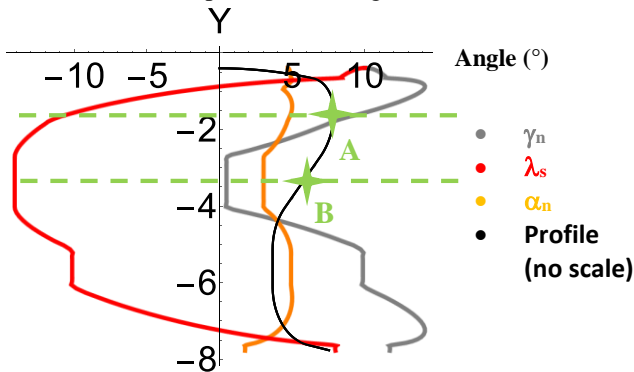


Fig. 7. Local cutting geometry all along a half tooth profile ( $\gamma_{n0} = \lambda_{s0} = 10^\circ$ ,  $A_f = 5^\circ$ ).

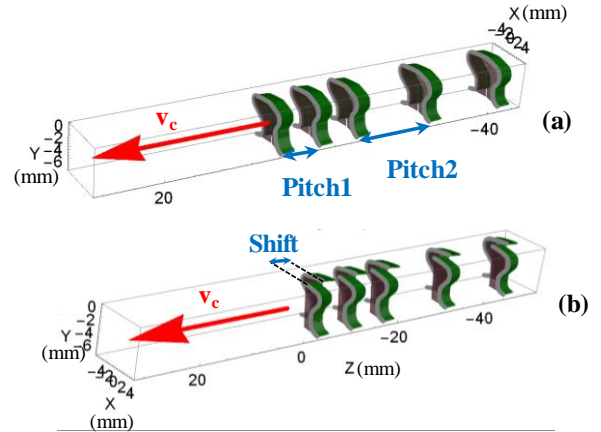


Fig. 8. Modelling of two broaches: without (a) and with (b) alternated half teeth.

At each broach position step, the location of the machined disk is calculated. Fig. 9 shows both planes of the workpiece.

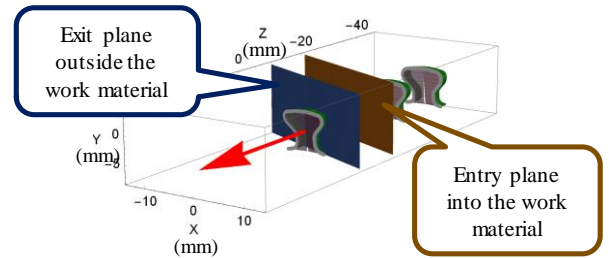


Fig. 9. Location of the part material.

At this point the geometrical model is able to calculate the local geometry all along the cutting edges of the half teeth and the engagement of the broach into the material.

### 3. Mechanistic model of the cutting forces

#### 3.1. The developed methodology

The cutting edge discretization method is used to calculate the global forces by summation of all the local ones applied on every segments of the discretization. The different steps to determine the forces applied on the tool are detailed on Fig. 10.

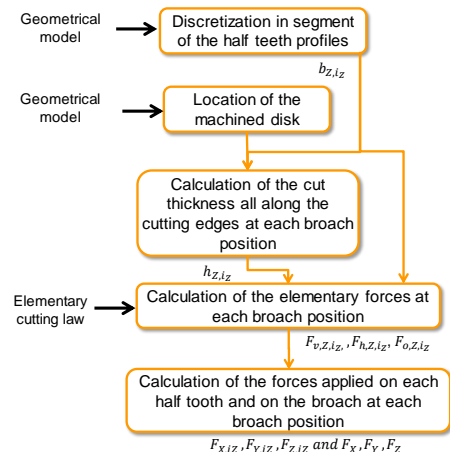


Fig. 10. Methodology to calculate the forces applied on the tool.

### 3.2. Calculation of the cut thickness

The cut thickness is considered to be the distance between the current point on its half tooth profile to another point of the half tooth profile that machined just before. The distance is measured in the reference plane (Pr) and perpendicularly to the current half tooth profile [10]. This methodology is explained on Fig. 11.

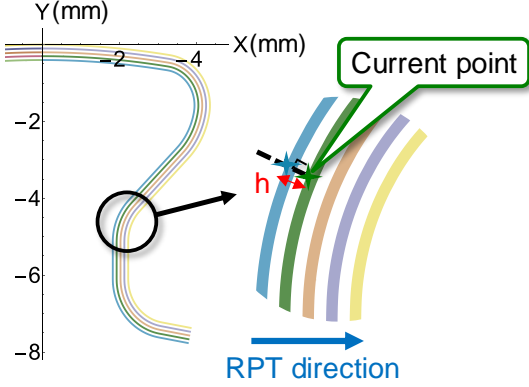


Fig. 11. Calculation of the cut thickness (h).

Only a broach for finishing operation is modelled. Thus, it is necessary to consider the machined profile by the rough broach. It is the blue profile in the Fig. 12.

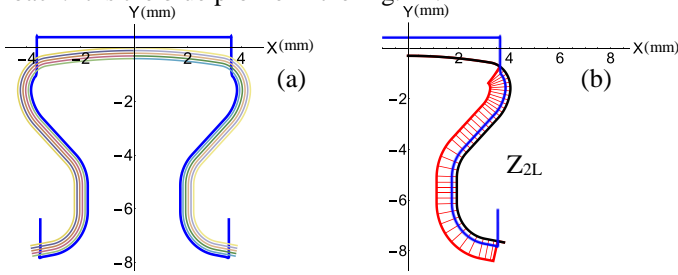


Fig. 12. (a) Definition of the broached profile before the current broach (blue). (b) Cut thickness (red) along the profile of one half tooth at one broach position.

So, the cut thickness is calculated considering the method presented in Fig. 11. But if the normal distance to the rough machined profile is shorter, this distance is considered to be the cut thickness.

### 3.3. Cutting law and force calculation

Initially a mechanistic cutting law with two force components has been used in the chip flow plane. The equation (1) law is chosen because it takes into account the local cutting geometry ( $\gamma_n$  and  $\alpha_n$ ) and allows to separate the forces linked to the edge and cut effects. This law is inspired by the work of Altintas [11]. The edge effect corresponds to the forces produced by the friction between the flank faces and the part and also the forces due to the edge radius. The cut effect is produced by the chip flow on the rake face (cf. equation (1) and Fig. 13).

The experiments have been done at constant speed. The cutting speed effects are taken into account by the constant parameters of the cutting law coefficients of equation (1).

The coefficients are determined thanks to experiments conducted during orthogonal cutting of the nickel based super-alloy.

$$\begin{aligned} F_v &= b(k_{0v} + k_{av}\alpha_n + k_{hv}(1 + k_{\gamma v}\gamma_n)h) \\ &= F_{v,edge} + F_{v,cut} \\ F_h &= b(k_{0h} + k_{ah}\alpha_n + k_{hh}(1 + k_{\gamma h}\gamma_n)h) \\ &= F_{h,edge} + F_{h,cut} \end{aligned} \quad (1)$$

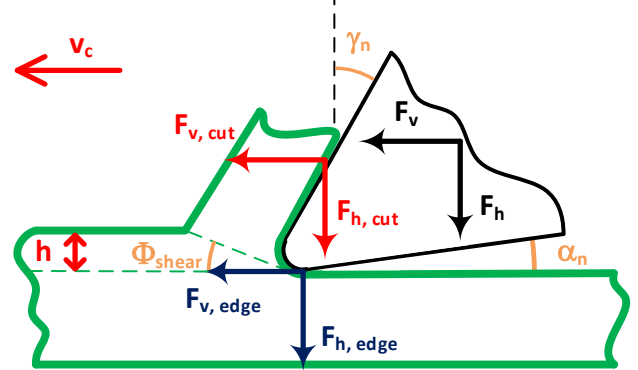


Fig. 13. Parametrization of the cutting forces for an orthogonal cutting operation.

However, each segment of the discretized cutting edges is not considered in orthogonal but in oblique cutting. A mechanical transformation described by Altintas [11] is used to transform the two components law to a three components one, considering the cutting edge inclination. Only the cut effect part of the law is affected (cf. equation (2) and Fig. 14 (b)).

$$\begin{aligned} F_v &= K_{v,cut}(\gamma_n, \lambda_s) \cdot b \cdot h + F_{v,edge}(\alpha_n) \\ F_h &= K_{h,cut}(\gamma_n, \lambda_s) \cdot b \cdot h + F_{h,edge}(\alpha_n) \\ F_o &= K_{o,cut}(\gamma_n, \lambda_s) \cdot b \cdot h \end{aligned} \quad (2)$$

The hypotheses are the following:

- $\lambda_s$  equals the chip flow angle,
- $\gamma_n, \text{oblique} = \gamma_n, \text{orthogonal}$ ,
- $\Phi_{shear, \text{oblique}} = \Phi_{shear, \text{orthogonal}}$ ,
- $\tau_s, \text{oblique} = \tau_s, \text{orthogonal}$  ( $v_c$  and  $h$  unchanged).

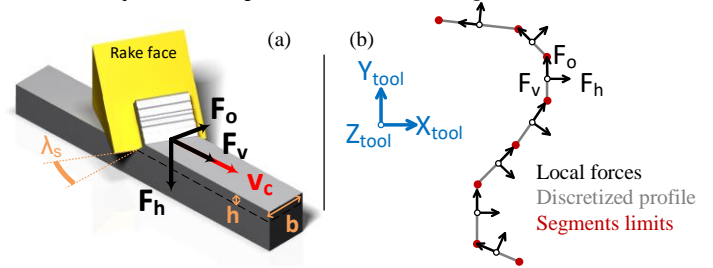


Fig. 14. Oblique cutting parametrization (a). Application to a half teeth profile (b).

Thus, for each segment of the discretized cutting edges, the width of cut, the chip thickness and the cutting geometry are well defined. Thanks to the cutting law equation (2), the forces applied on each segment can be determined in a coordinate system linked to the segment orientation for each position step of the broach (cf. Fig. 14 (b)). A change of basis is necessary to have all the local forces in the same basis linked to the tool coordinates system (cf. equation (3)).

Then, the forces applied on each segment of each cutting edge are summed on equation (4).



$$\begin{pmatrix} F_{x,is,iZ_{ab}} \\ F_{y,is,iZ_{ab}} \\ F_{z,is,iZ_{ab}} \end{pmatrix} = M_{i,iZ_{ab}} \begin{pmatrix} F_{v,is,iZ_{ab}} \\ F_{h,is,iZ_{ab}} \\ F_{o,is,iZ_{ab}} \end{pmatrix} \quad (3)$$

Where:

- $M_{i,iZ_{ab}}$ : the transformation matrix,
- $is$ : the segment index,
- $iZ_{ab}$ : the half tooth index.

$$\begin{pmatrix} F_{x,iZ_{ab}} \\ F_{y,iZ_{ab}} \\ F_{z,iZ_{ab}} \end{pmatrix} = \sum_{is=1}^{\text{Number of segments}} \begin{pmatrix} F_{x,is,iZ_{ab}} \\ F_{y,is,iZ_{ab}} \\ F_{z,is,iZ_{ab}} \end{pmatrix} \quad (4)$$

To obtain the forces applied on the tool for each step of position, the forces applied on all the half teeth are summed on equation (5).

$$\begin{pmatrix} F_x \\ F_y \\ F_z \end{pmatrix} = \sum_{iZ_{ab}}^{\text{Number of half teeth}} \begin{pmatrix} F_{x,iZ_{ab}} \\ F_{y,iZ_{ab}} \\ F_{z,iZ_{ab}} \end{pmatrix} \quad (5)$$

## 4. Results of the parametrized model

### 4.1. The results of the model

The cutting forces simulation results of a broaching operation are presented on Fig. 15. The parameters are:

- $\gamma_{n0} = 10^\circ$  and  $\lambda_{s0} = 10^\circ$ ,
- $A_f = 5^\circ$ ,  $A_g = 10^\circ$  and  $70^\circ$ ,
- Shift = 0 mm: not alternated,
- Pitch1 = 7 mm and Pitch2 = 14 mm,
- WPi =  $15^\circ$ ,
- Disk thickness = 10 mm.

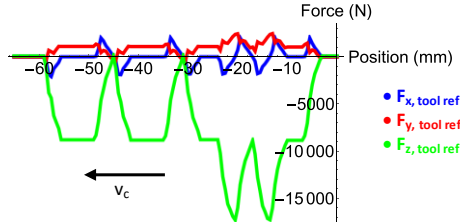


Fig. 15. Results of the modelling.

The software used is Wolfram Mathematica 11.1. The calculation time (for geometrical and mechanistic model) is around 10 minutes with 100 elements on each half teeth profile.

The results show that the force on the X axis is not equal to zero and the sign changes during the broaching operation. This is due to the angle between the tool axis and the part axis. The pairs of half teeth do not enter into the material at the same time. The value of the pitch has an impact on the magnitude of Fy and Fz forces. The first pitch which is the shorter implies higher values than the second one. It depends of the number of half teeth simultaneously inside the part.

### 4.2. Global parameters effect

Three other simulations are presented in Fig. 16 with a smaller rake face orientation to present the global parameters

effects. The workpiece inclination induces unbalance forces along the X axis. If the inclination is equal to zero, Fx equals to zero during broaching as shown on Fig. 16 (a) and (b).

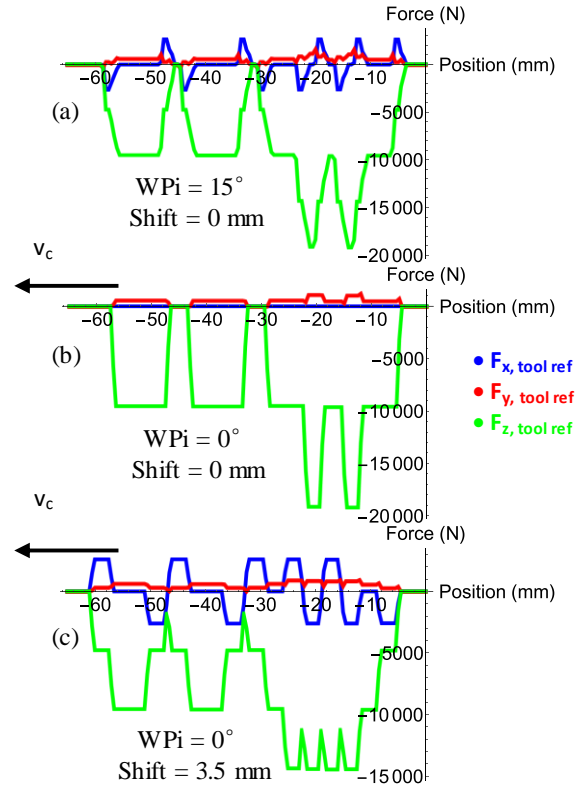


Fig. 16. Influence of the workpiece inclination and the half teeth shift. Constant parameters: Disk thickness = 10 mm, Pitch1 = 7 mm, Pitch2 = 14 mm,  $\gamma_{n0} = 5^\circ$  and  $\lambda_{s0} = 5^\circ$ .

It is possible to adjust the half teeth shift value to increase the cutting continuity. Fig. 16 (c) shows that Fz force variation are limited compared to Fig. 16 (b). Nevertheless, it induces an unbalance of Fx force due to the shift between the half teeth of each pair.

### 4.3. Cutting geometry effect

Four simulations are presented in Fig. 17 and Fig. 18 to show the influence of the variation of the rake face orientation, i.e. the change of the  $\gamma_{n0}$  and  $\lambda_{s0}$  values. Fig. 17 presents the effect of the rake face orientation on the cutting geometry variation.

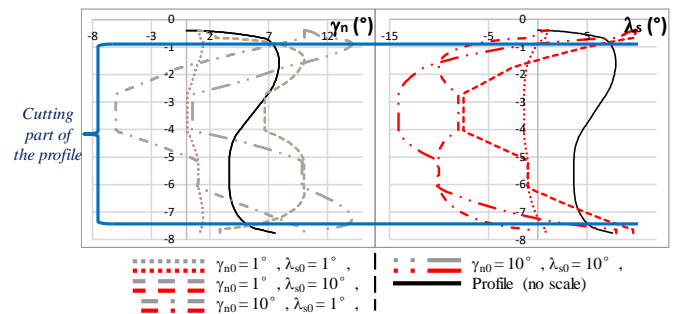


Fig. 17. influence of the variation of the rake face orientation on the local cutting geometry of a half tooth profile

The shape and values of the local geometry essentially depend on the rake face orientation and the cutting forces as well, as shown on Fig. 18.

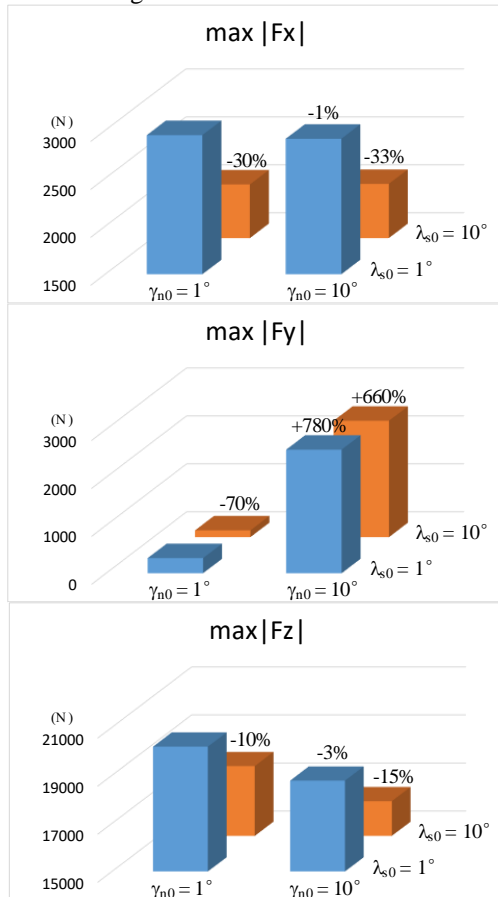


Fig. 18. Effect of  $\gamma_{n0}$  and  $\lambda_{s0}$  on the cutting forces. The reference of the percentages is  $\gamma_{n0} = 1^\circ$  and  $\lambda_{s0} = 1^\circ$ .

The case  $\gamma_{n0} = 10^\circ$  and  $\lambda_{s0} = 1^\circ$  induces negative  $\gamma_n$  angles on a part of the cutting edge. The cutting law coefficients have not been identified on this range. The results given are an estimation.

Fig. 18 shows that if  $\gamma_{n0}$  and  $\lambda_{s0}$  increase, the  $F_z$  cutting force decreases. It is consistent with the experimental results.

The impact of  $\gamma_{n0}$  and  $\lambda_{s0}$  are different on  $F_x$ ,  $F_y$  and  $F_z$  forces. A change of the  $\gamma_{n0}$  value has an important impact on  $F_y$  but not on the other components. This can partly be explained by the increase of the  $\lambda_s$  angle on the half teeth sides, which are also the main portions on the cutting edges that cut, when the  $\gamma_{n0}$  angle increases (cf. Fig. 17).  $F_x$  and  $F_z$  are more influenced by the  $\lambda_{s0}$  increase because it implies higher  $\gamma_n$  values on the half teeth sides (cf. Fig. 17).

## 5. Conclusion

This article presents a methodology that allows to model the cutting geometry of a broach with complex shape and to estimate the involved cutting forces.

The geometrical parameters of the proposed generalized model are numerous to adapt the calculation to various broach design:

- Final slot profile,
- Rake face orientation (with  $\gamma_{n0}$  and  $\lambda_{s0}$ ),
- Flank face definition (with  $A_f$  and  $A_g$ ),

- Two different pitches,
- Alternation or not of the half teeth.

The first results allow to understand the effect of the rake face orientation on the local cutting geometry and on the cutting forces. The three components of the cutting forces are not influenced in the same way by the change of  $\gamma_{n0}$  or  $\lambda_{s0}$  angles. In our example the change of the  $\gamma_{n0}$  angle will have a significant effect on the  $F_y$  force but not on  $F_x$  and  $F_z$ . The modification of the  $\lambda_{s0}$  angle will have an opposite effect. The choice of the rake face orientation on a production broach results of a compromised.

Some outlooks could be the definition of non-constant rise per tooth all along the cutting edges and the study of the global chip flow directions.

## 6. Bibliography

- [1] D. Fabre, C. Bonnet, J. Rech, and T. Mabrouki. Optimization of surface roughness in broaching. *CIRP J. Manuf. Sci. Technol.* 2017; 18: 115–127.
- [2] A. J. P. Sabberwal. Chip section and cutting force during the milling operation. *Ann. CIRP* 1961; 10(3): 197–203.
- [3] E. J. A. Armarego. Unified-generalized mechanics of cutting approach - a step towards a house of predictive performance models for machining operations. *Mach. Sci. Technol.* 2000; 4(3): 319–362.
- [4] S. Campocasso, J.-P. Costes, G. Fromentin, S. Bissey-Breton, and G. Poulachon. A generalised geometrical model of turning operations for cutting force modelling using edge discretisation. *Appl. Math. Model.* 2015; 39(21):6612–6630.
- [5] M. Kaymakci, Z. M. Kilic, and Y. Altintas. Unified cutting force model for turning, boring, drilling and milling operations. *Int. J. Mach. Tools Manuf* 2012; 54–55: 34–45.
- [6] A. Molinari and A. Moufki. A new thermomechanical model of cutting applied to turning operations. Part I. Theory. *Int. J. Mach. Tools Manuf* 2005; 45(2): 166–180.
- [7] P. Vogtel, F. Klocke, H. Puls, S. Buchkremer, and D. Lung. Modelling of Process Forces in Broaching Inconel 718. *Procedia CIRP* 2013; 8: 409–414.
- [8] P. Vogtel, F. Klocke, D. Lung, and S. Terzi. Automatic Broaching Tool Design by Technological and Geometrical Optimization. *Procedia CIRP* 2015; 33: 496–501.
- [9] G. Fromentin and G. Poulachon. Geometrical analysis of thread milling-part 1: Evaluation of tool angles. *Int. J. Adv. Manuf. Technol.* 2010; 49(1–4): 73–80.
- [10] G. Fromentin and G. Poulachon. Geometrical analysis of thread milling-part 2: Calculation of uncut chip thickness. *Int. J. Adv. Manuf. Technol.* 2010; 49(1–4):81–87.
- [11] Y. Altintas, *Metal Cutting Mechanics, Machine Tool Vibrations, and CNC Design*. Cambridge university press; 2000.